

# Transparent Colored Display Enabled by Flat Glass Waveguide and Nanoimprinted Multilayer Gratings

Zeyang Liu, Qingyu Cui, Zhanhua Huang, and L. Jay Guo\*

Cite This: *ACS Photonics* 2020, 7, 1418–1424

Read Online

ACCESS |



Metrics &amp; More



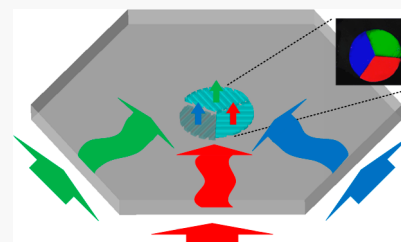
Article Recommendations



Supporting Information

**ABSTRACT:** In this paper, a type of transparent colored static display consisting of a flat glass waveguide and embedded multilayer gratings is presented, by which multiple patterns and colors with a wide field of view (FOV) can be displayed. The embedded grating is achieved by nanoimprinting followed by deposition of a high refractive index dielectric layer. The process can be repeated to produce multilayer gratings, which are shaped into specific patterns to be displayed, and they are designed to have proper periods and orientations to independently extract light incident from different edges of the glass plate. Such transparent display offers the advantages of low cost, easy fabrication and wide FOV, and it is suitable for colored signage and decorative applications.

**KEYWORDS:** waveguide display, transparent display, multicolor display, nanoimprint lithography, multilayer gratings



Transparent display has long been an extensively studied area that draws keen interests of the public. It has broad applications in many fields, especially in mobile display, wearable devices and heads-up displays in automobiles. With the help of transparent display, information can be shown and observed without blocking the background, presenting minimum intrusion to the normal field of view. Several approaches have been proposed and developed to realize transparent display, including fluorescent molecules that emit visible light when excited by invisible UV or infrared light,<sup>1–4</sup> organic light emitting diodes (OLEDs) with transparent electrodes,<sup>5–7</sup> diffusive screens,<sup>8</sup> and nanoparticle-enabled displays<sup>9</sup> based on narrow band light scattering. Although each method has its unique advantages suitable for certain applications, the drawbacks still exist. For instance, fluorescent molecules demand high-energy conversion efficiency, which is hard to achieve for all colors; the cost and lifetime of transparent OLEDs restrict them to have broader applications; for diffusive screens or nanoparticle-enabled displays, reduced transparency or even colored tones resulting from light scattering need to be improved. Apart from the above approaches, waveguide display is another promising method. It generally comprises two components: a flat waveguide made of glass or polymer to guide light by total internal reflection (TIR) and couplers to extract light from the waveguide by interrupting the TIR condition. The waveguide display was originally proposed for wearable augmented reality (AR) displays,<sup>10–14</sup> because it can transfer light from the image source to the eye box using transparent optical elements. Following that, D. Fattal et al. divided the out-coupling grating to carefully designed grating pixels with different periods and orientations, so as to diffract the guided light to different fields of view (FOVs), realizing a wide-angle, glasses-free transparent

3D display.<sup>15</sup> However, as it relies on pixelated gratings, scaling up to a large display area remains challenging.

Here, we develop the waveguide display configuration by using multilayer gratings and implement a type of transparent colored signages to demonstrate its principle. The device is made on a piece of shaped flat glass with all edges polished for light input. Grating of each layer is designed to have a proper period and orientation as well as a specific pattern; therefore, it can independently out-couple the guided light incident from the corresponding edge and enables the device to display multiple patterns and colors with a wide FOV. In this work, we demonstrate three types of device configurations, with single-layer grating, two-layer gratings, and three-layer gratings fabricated on rectangular or hexagonal shaped glass. The multilayer gratings are embedded in UV-curable polyurethane acrylate (PUA) resin and are fabricated by repeating nanoimprint lithography<sup>16,17</sup> using the corresponding grating molds and electron beam evaporation of titanium dioxide (TiO<sub>2</sub>) after each imprinting. The FOV and the display area are investigated by tracing out-coupled light backward. Two methods to enlarge the FOV are also proposed and demonstrated. This type of transparent display offers the advantages of low cost, easy fabrication, and wide FOV, and it is suitable for colored signage and decorative applications.

Received: December 20, 2019

Published: May 11, 2020



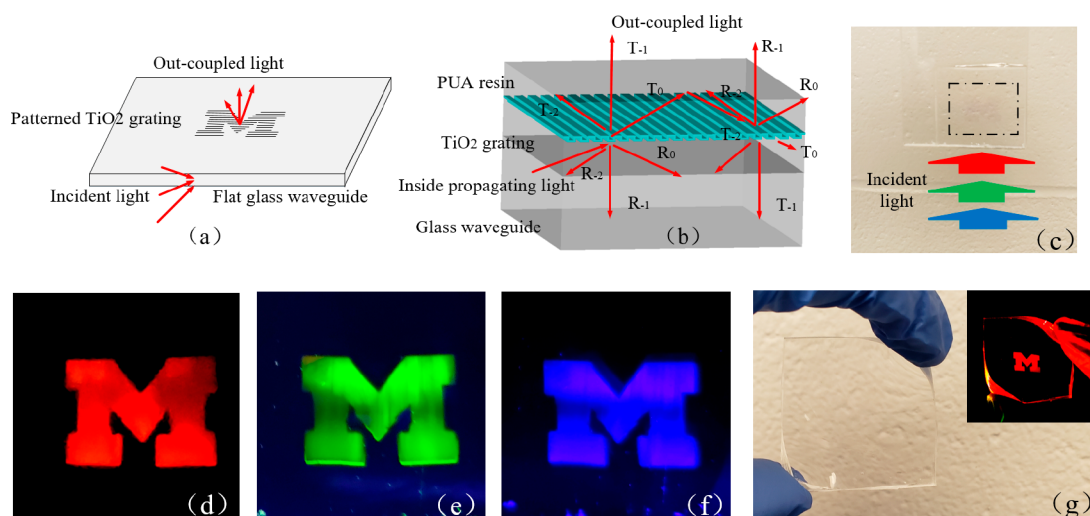


**Figure 1.** (a) Schematic diagram of the transparent display comprising a flat glass waveguide and a patterned grating. (b) Diffraction order distribution of the propagating light inside the glass waveguide. (c) Rectangular flat glass with a single-layer embedded  $\text{TiO}_2$  grating appears transparent. When light of different colors is incident from the bottom edge, the letter M is displayed as (d) red, (e) green, and (f) blue on the glass. (g) A flexible colored pattern is demonstrated by a PDMS-based device. The rectangle flat glass is 8 cm  $\times$  5 cm, with a thickness of 4 mm. The display area denoted by the dashed rectangle is about 3 cm  $\times$  2 cm.

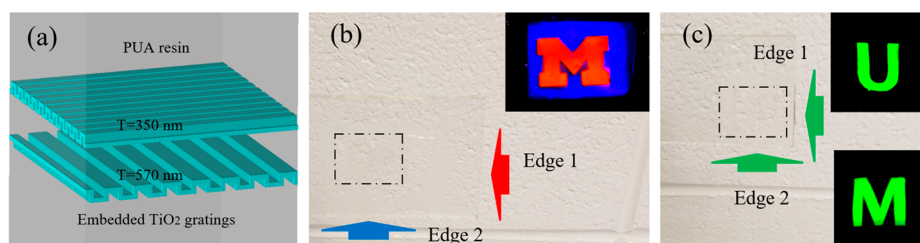


**Figure 2.** (a) Two-layer embedded  $\text{TiO}_2$  gratings with mutually perpendicular grooves. (b) Sample 1: a “M” pattern in one layer and its complementary shaped pattern in the other layer. When blue light and red light are input into the glass from the two adjacent edges simultaneously, a dual-color pattern is lit up. (c) Sample 2: the two layers of gratings fabricated on the flat glass are shaped in two independent letter patterns “U” and “M”, which can be selectively displayed by changing the edge of light incidence. The dashed rectangle denotes the display area with a size of around 3 cm  $\times$  2 cm.

### ■ THREE CONFIGURATIONS AND EXPERIMENTAL RESULTS

The proposed waveguide display consists of a piece of edge-polished flat glass and multiple-layer patterned gratings on the top surface of the glass. The working principle is illustrated by Figure 1a,b. Light emitted from a backlight panel is directly input into the flat glass from the edge. The flat glass acts as a waveguide to propagate light by TIR. When the inside light meets the grating on the top surface, diffraction occurs and splits light into several beams. Light in the first diffraction orders ( $R_{-1}$  and  $T_{-1}$ ) exits the waveguide while light in the zeroth order keeps propagating along the same direction, and it will be diffracted again after being bounced back from the top surface. To implement a signage, the grating region is shaped to a desired pattern, and the guided light can only get out from the patterned area, making the pattern visible on the transparent glass. Moreover, because the inside propagating light is not collimated and it has randomly distributed angles, the displayed pattern can be seen from a broad angular range, which can be calculated by the grating equations discussed in section 3. The patterned gratings are embedded in UV-curable PUA resin and they are made of  $\text{TiO}_2$ .

Because all the materials used to fabricate the device are transparent, when no light is incident, the entire glass

waveguide has good transparency, as shown in Figure 1c. As the grating can diffract visible light of any wavelength, the pattern can show different colors depending on the wavelength of the incident light. The experimental results are presented in Figure 1d–f. Moreover, because the incident light can be guided by a curved waveguide, a flexible colored pattern can be realized when a flexible polymer waveguide is employed, as demonstrated by the device shown in Figure 1g, which is made of PDMS.

Although the pattern in Figure 1 can show different colors, it is still monochromatic. To make the pattern display more colors, multiple light sources of different wavelength are placed at different edges and multilayer gratings are employed to diffract light incident from the corresponding edges. To achieve this, the grooves of the multilayer gratings are oriented parallel to the corresponding edges. The angle of the first order diffracted light is determined by the grating vector, which is inversely proportional to the period and is perpendicular to the groove. By carefully designing the periods and orientations of the gratings, the light propagating inside the glass from different edges can only be extracted by the corresponding grating coupler. Therefore, multiple colors can be displayed without crosstalks. Moreover, if the gratings in different layers are shaped into independent patterns, these patterns can be selectively displayed. Two samples using rectangular flat glass

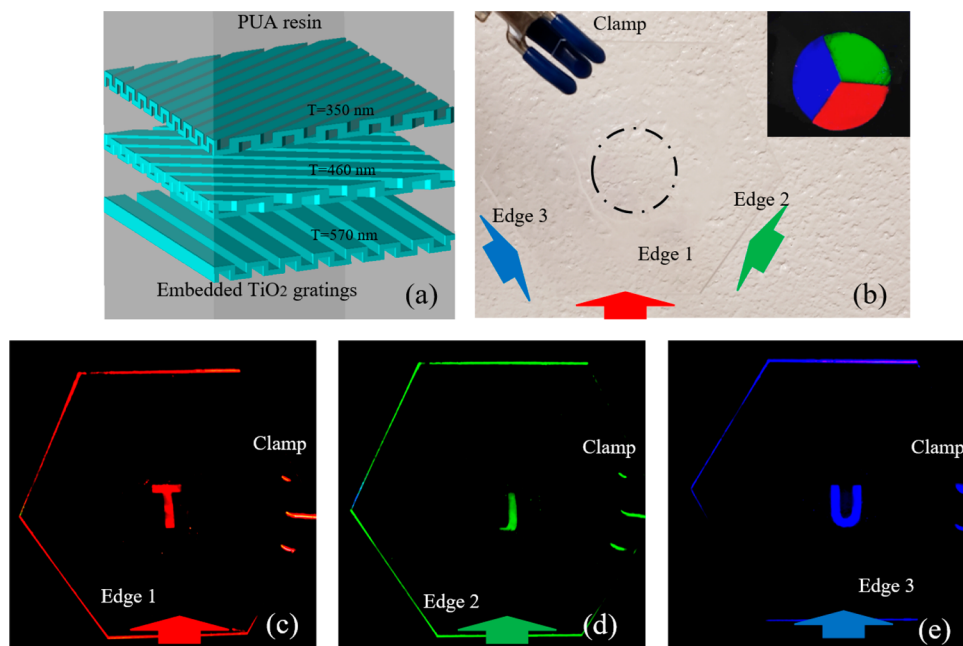


**Figure 3.** (a) Three-layer embedded  $\text{TiO}_2$  gratings whose grooves in different layers are oriented  $120^\circ$  from each other and parallel to the corresponding edges. (b) Sample 1: a R, G, B-colored circular pattern consisting of three-layer fan-shaped grating zones is displayed on the transparent glass with simultaneous red, green, and blue light incidence from the corresponding edges. (c–e) Sample 2: Three letter patterns “T”, “J”, and “U” in different colors can be selectively shown in the same location of the glass waveguide when red, green, and blue light is input from the corresponding edges, respectively. The hexagonal flat glass has a side length of 4.5 cm and a thickness of 2 mm. The dashed circle denotes the display area with a diameter of 3 cm.

with two-layer gratings are presented. The first sample in Figure 2b has two mutually complementary patterns, making up a red “M” on a blue background. Figure 2c shows two separate patterns, the letters “U” and “M” on the same glass, which can be selectively displayed by inputting light from different edges.

The same principle also works for a hexagonal shaped waveguide, where three layers of gratings corresponding to three adjacent edges can be stacked on the center of the glass to display more patterns and colors. The period of the grating in each layer is 350, 460, and 570 nm, respectively, which is approximately proportional to the design wavelength (420 nm for blue, 532 nm for green, and 630 nm for red, determined by the color filters used in the experiment). The grooves of the gratings in different layers are parallel to the corresponding edges. Two samples using hexagonal shaped glass with three-layer gratings are fabricated, and the experimental results are presented in Figure 3b–e. As shown, no crosstalks between patterns or colors occur. All designed patterns are displayed independently.

As different colors can be independently displayed by gratings with different period and orientations, mixed colors can be formed by pixelating the gratings<sup>15</sup> or overlapping the multilayer gratings. We demonstrated a three-color pattern by two-layer partially overlapped gratings. The yellow color shows up in the overlapped area with red and green light input, as shown in the Supporting Information.

### FOV AND DISPLAY AREA

The FOV and the display area corresponding to the maximum FOV are important parameters for evaluating the performance of the proposed transparent display. We adopt a backward ray-tracing strategy to estimate the maximum FOV and the display area. The backward ray tracing reverses the light propagation

direction by treating the out-coupled light as incident light and traces it from the grating to its source at the input edge, as shown in Figure 4. Grating equations are derived as below and are used to calculate the diffraction angles. In the diffraction geometry, the K-vector of the incident light is

$$k_i = \frac{2\pi}{\lambda} n_0 (\sin \theta_i \cos \varphi_i, \sin \theta_i \sin \varphi_i, \cos \theta_i) \quad (1)$$

and the K-vector of the  $m$ th diffracted order in the glass is

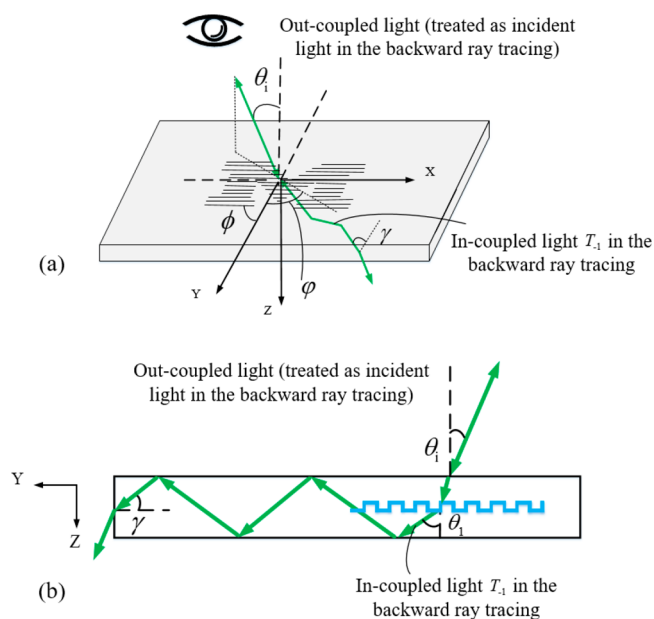


**Figure 4.** Schematic diagrams in (a) 3D view and (b) side view of the backward ray tracing.

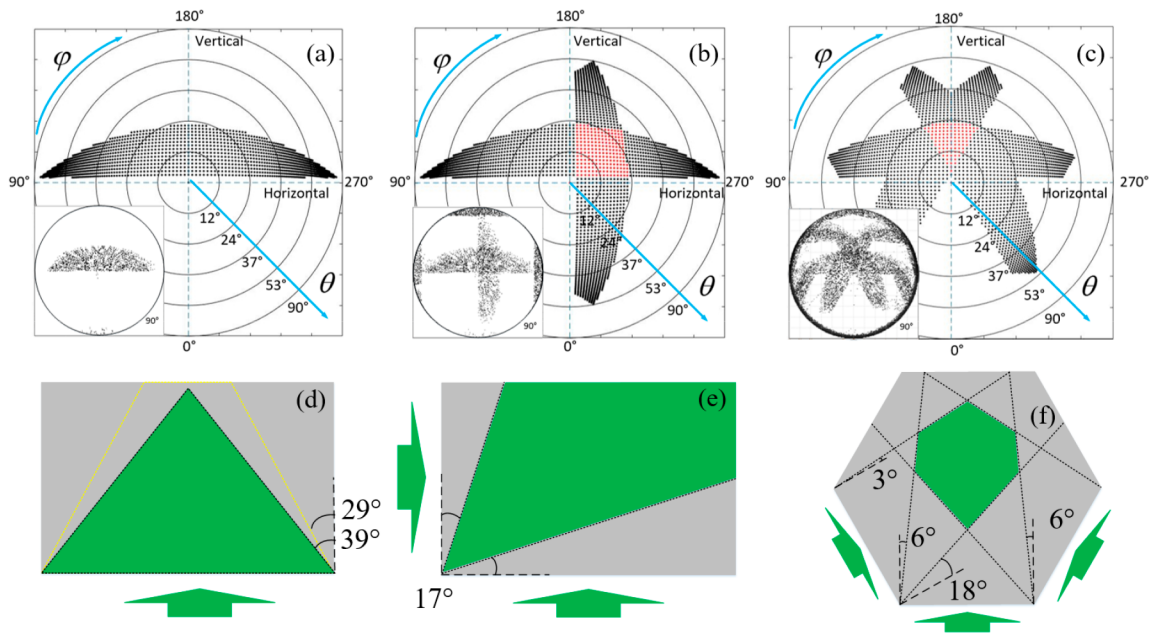


**Figure 5.** (a–c) Calculated FOV maps of different patterns/colors. The overlapped dots (colored red) represent the CFOVmax, among which all patterns and colors can be seen. (d–f) Display areas corresponding to the CFOVmax of different configurations. The insets of parts a–c show the simulation results of FOVs, which agree well with the calculation. The arrows in parts d–f indicate the edges of the incidence.

$$k_m = \frac{2\pi}{\lambda} n_1 (\sin \theta_m \cos \varphi_m, \sin \theta_m \sin \varphi_m, \cos \theta_m) \quad (2)$$

where  $\lambda$  is the wavelength of the incident light and  $m$  is the order of diffraction.  $n_0$  and  $n_1$  are the refractive indices of air and the waveguide material, respectively. The grating equations in the conical geometry are

$$\begin{aligned} n_1 \sin \theta_m \sin \varphi_m &= n_0 \sin \theta_i \sin \varphi_i + m \frac{\lambda}{T} \cos \phi \\ &= \gamma + m \frac{\lambda}{T} \cos \phi \\ n_1 \sin \theta_m \cos \varphi_m &= n_0 \sin \theta_i \cos \varphi_i + m \frac{\lambda}{T} \sin \phi \\ &= \alpha_0 + m \frac{\lambda}{T} \sin \phi \end{aligned} \quad (3)$$

where  $T$  is the period of the grating in-coupler.  $\theta$ ,  $\varphi$ , and  $\phi$  are the incident angle, the azimuth angle of incidence plane, and the angle between grating grooves and the  $Y$  axis, respectively. Derived from eq 3, the diffraction angle of the first order can be expressed by the following equations:

$$\begin{aligned} \varphi_1 &= \arctan \left[ \left( \gamma + \frac{\lambda \cos \phi}{T} \right) / \left( \alpha_0 + \frac{\lambda \sin \phi}{T} \right) \right] \\ \theta_1 &= \arcsin \left( \frac{\gamma + \lambda \cos \phi / T}{n_0 \sin \varphi_1} \right) \end{aligned} \quad (4)$$

In the backward ray-tracing, two TIR related conditions must be satisfied to make sure the incident light can reach its source at the polished edge of the glass. First, the angle of the first diffraction order  $\theta_1$  should be larger than the critical angle of TIR to ensure the first order be restricted within glass. Second,

the incident angle  $\gamma$  of the in-coupled light on the polished surface of the corresponding edge, which can be expressed as  $\arctan(\sqrt{(\tan^2 \theta_1 + 1/\tan^2 \varphi_1 + \tan^2 \theta_1/\tan^2 \varphi_1)})$ , should be smaller than the critical angle of TIR such that the in-coupled light can be refracted out from the polished edge. Under the above two conditions and the given parameters including the grating period, wavelength, and the refractive index of glass ( $\sim 1.46$ ), the maximum FOV and the corresponding display area can be calculated. Due to the high intensity contrast between the zeroth order and other diffraction orders, we only consider the primary diffraction and ignore the following secondary diffraction of other orders. The calculation results of the maximum FOV and the display area for the rectangular flat glass with a single-layer grating are presented in Figure 5a,d, which agree well with the simulation implemented by TracePro, as shown in the inset. The FOV is approximately from  $-70^\circ$  to  $70^\circ$  horizontally and  $2^\circ$  to  $21^\circ$  vertically. Wider horizontal FOV results in larger angular divergency of the in-coupled light; hence, there is a trade-off between the display area and the horizontal FOV. A larger display area (dashed yellow trapezoid) is also shown as a comparison when a smaller horizontal FOV from  $-40^\circ$  to  $40^\circ$  is needed. By applying these two TIR conditions to more layers of gratings and more edges, the maximum FOV and the display area of the other two configurations can also be obtained, as shown in Figure 5b,c,e,f. The ratio between the wavelengths and the corresponding periods of gratings for light in different colors is fixed to 1.16 according to the nanoimprint molds and the filters used in experiment. The redundant dots at the edges of the simulated FOV maps are caused by stray light, which has two sources: the higher orders ( $|m| > 1$ ) in the diffraction of corresponding grating or it is generated in the diffraction of noncorresponding gratings. However, because of its very large angle, the stray light will not affect the normal display and can be neglected. The overlapped dots (colored red) in the FOV maps represent the angles of out-coupled light in which all

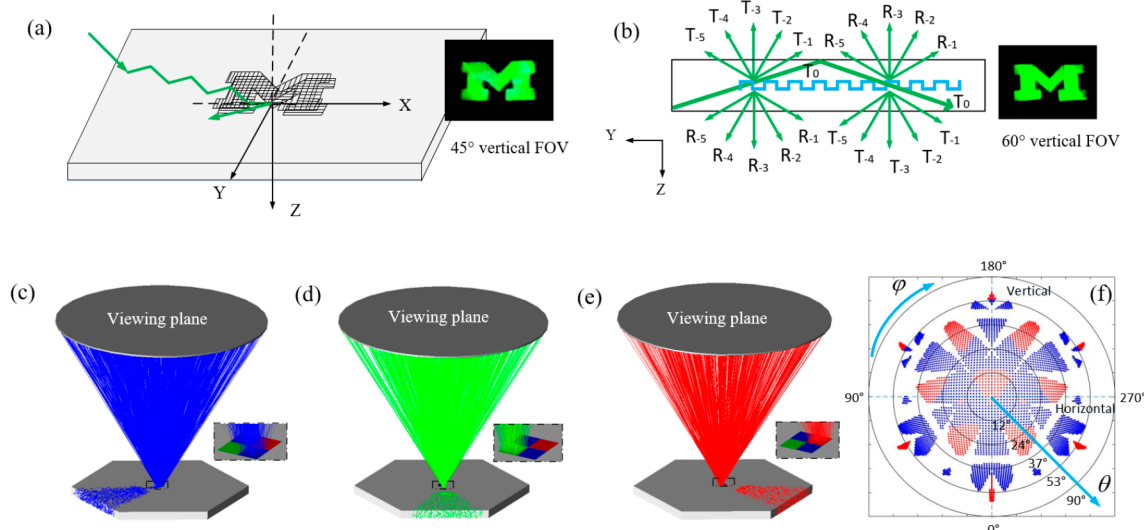


**Figure 6.** (a) Two-layer gratings on rectangular flat glass with overlapped patterns. (b) Diffraction order distribution when 1220 nm period grating diffracts green light (532 nm), leading to a broader angular range of the out-coupled light in the vertical direction. Insets of parts a and b present the photos of patterns taken from a vertical FOV, 45° and 60°, respectively. (c–e) Ray-tracing simulation results of the hexagonal flat glass with spatially separated longer period gratings. The grating period corresponding to the blue, green, and red light is 963 nm, 1220 nm, and 1445 nm, respectively. The grooves of the grating pixels are parallel to the corresponding edges. The insets of parts c–e are the enlarged views of the grating pixels, showing independent out-coupling. (f) Calculated CFOVmax of the hexagonal shaped flat glass with three-layer longer period gratings, which is represented by the red dots. The CFOVmax is expanded to all the dots when the number of layers increases to six with periods of 963 and 805 nm for blue light, 1220 and 1020 nm for green light, 1445 and 1208 nm for red light.

patterns and colors can be seen, namely, the maximum common FOV (CFOVmax). The display area where patterns should be fabricated to have CFOVmax is colored green in Figure 5e,f, which is delimited by the azimuth angles  $\varphi_1$  of in-coupled light. When the incident angle varies within the range of CFOVmax, for the rectangular glass with two-layer gratings, the azimuth angle  $\varphi_1$  ranges from 1° to 17°; for the hexagonal shaped glass with three-layer gratings, azimuth angle  $\varphi_1$  ranges from -6° to 6° for the bottom edge and ranges from 3° to 18° for the other two adjacent edges, respectively. The ranges of azimuth angles  $\varphi_1$  also indicate that light in-coupled by different gratings can only propagate to the corresponding edges, which explains the independent control of patterns/colors. It should be noted that the display area shown here corresponds to the CFOVmax for all patterns/colors, while other parts outside the green area can also display but with a smaller or larger FOV for different patterns/colors.

## ■ TWO METHODS TO ENLARGE THE FOV

When the grooves of grating are horizontally oriented, the horizontal FOV is much wider than the vertical one, as illustrated in Figure 5a. Here, we introduce two methods that can remarkably enlarge the vertical FOV. The first one is adopting multilayer gratings, where the patterns of different layers are the same and overlapped, such that the pattern can be seen when the inside light is out-coupled by either grating. Therefore, the FOV is expanded to all the dots instead of the overlapped ones, as shown in Figure 5b,c. We fabricated a sample with two-layer gratings in overlapped patterns. As expected, the pattern is still visible when the vertical FOV increases to  $\pm 45^\circ$ , as presented in the inset of Figure 6a. The FOV can be further expanded in other directions if more layers of gratings with different orientations are stacked.

The other method is to take the advantage of higher diffraction orders by using a grating with a longer period. More

diffraction orders are generated when the light propagating inside the glass interacts with a longer period grating, leading to a broader angular range of out-coupled light. The period of the grating shown in Figure 6b is 1220 nm, enlarging the vertical FOV to over  $\pm 60^\circ$ . Fortunately, the longer period gratings used to achieve a broader FOV can still be independently controlled to display multiple patterns and colors by aligning their grooves parallel to the corresponding edges. The ray-tracing simulation results are presented in Figure 6c–e. The gratings with periods of 963 nm, 1220 nm, and 1445 nm for blue, green, and red light, respectively, are spatially separated on the surface of the glass plate for ease of demonstration. Light only exits the waveguide from the corresponding grating area, showing the ability to independently display multiple patterns and colors. The red dots in Figure 6f represent the calculated CFOVmax of the hexagonal shaped waveguide with three-layer longer period gratings, which distributes over several islands due to the angular separation of different orders. Because of the discontinuity of the CFOVmax, certain patterns/colors cannot be seen when the FOV changes in the gaps between the red dot islands. This issue can be addressed by adding more layers of gratings to generate diffraction orders that can fill the gaps. When the number of grating layer increases to 6, with two layers for each pattern/color (963 and 805 nm for blue light, 1220 and 1020 nm for green light, 1445 and 1208 nm for red light), the separate islands of red dots are connected by the blue dots, showing a much broader CFOVmax compared with that of the similar configuration in Figure 5c.

## ■ SUMMARY

In summary, we demonstrate a type of static transparent display consisting of a flat glass waveguide and multilayer gratings. The grating in each layer has a proper period and orientation to only extract light incident from the correspond-

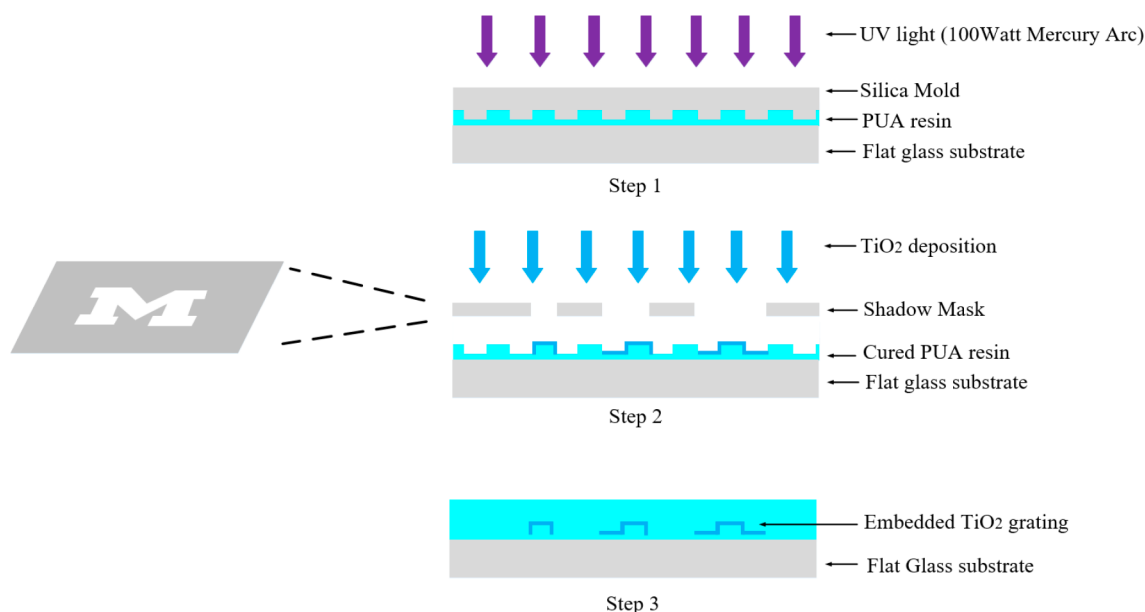


**Figure 7.** Fabrication process of the embedded TiO<sub>2</sub> grating.

ing edge by diffraction, enabling the device to display multiple patterns and colors. Nanoimprint and subsequent electron beam deposition of high index dielectrics are utilized repeatedly to fabricate the embedded multilayer patterned gratings. The FOV and the corresponding display area of three configurations are investigated and two approaches to enlarge the FOV are discussed and demonstrated. This design can be extended to flat glass with more edges to display more patterns and colors if desired; however, it will have a smaller CFOVmax. The advantages of low cost, easy fabrication, and wide FOV make this design promising to find wide applications in colored signage and decorative applications. Although the patterns demonstrated here are static, they can also be dynamic and achieve full-color display if electronically switchable gratings, such as by using liquid crystal etc., are adopted and pixelated to independently control different parts of the patterns. Moreover, as the hexagonal-shaped glass waveguide design can circumvent the dispersion nature of grating to independently control different colors, it can be further developed to realize a full-color AR waveguide display by, respectively, in-coupling red, green, and blue image-bearing light by gratings at three adjacent edges and out-coupling the composed full-color light from the center.<sup>11–13</sup>

## METHODS

The fabrication process is straightforward and illustrated in Figure 7: first, a silica mold (570 nm, designed for red light) is used to imprint the grating onto the PUA resin which is subsequently cured by UV light for 3 min. Then 80 nm thick TiO<sub>2</sub> film is deposited on the grating by electron beam evaporation, during which a shadow mask with the designed pattern is used to shape the deposited TiO<sub>2</sub> film; finally, another PUA layer is spin-coated and cured to eliminate the imprinted grating topography outside the patterned region, thereby forming the embedded patterned TiO<sub>2</sub> grating. The refractive index contrast between TiO<sub>2</sub> (around 2.2 in the visible without annealing) and cured PUA (around 1.5) enables the diffraction.

The fabrication of the multilayer gratings is repeating the process described above to stack different gratings. Grating with the designed period is imprinted sequentially on top of the PUA coating that planarizes the previous embedded TiO<sub>2</sub> grating, with a rotation of 90°/ 60° with respect to the previous layer, as shown in Figure 2a and 3a. A shadow mask with the designed pattern is covered on the surface of the grating in the following electron beam evaporation of TiO<sub>2</sub> after each imprinting to shape the TiO<sub>2</sub> grating responsible for diffracting the light. The fabrication process of the PDMS-based device is described in the Supporting Information, which is similar to that of the glass-based devices.

## ASSOCIATED CONTENT

### Supporting Information

The Supporting Information is available free of charge at <https://pubs.acs.org/doi/10.1021/acsphotonics.9b01803>.

Fabrication process of the PDMS-based flexible device, polarization of out-coupled light, and mixed colors by multilayer gratings (PDF)

## AUTHOR INFORMATION

### Corresponding Author

L. Jay Guo – Department of Electrical Engineering and Computer Science, University of Michigan, Ann Arbor, Michigan 48109, United States; [orcid.org/0000-0002-0347-6309](https://orcid.org/0000-0002-0347-6309); Email: [guo@umich.edu](mailto:guo@umich.edu)

### Authors

Zeyang Liu – Department of Electrical Engineering and Computer Science, University of Michigan, Ann Arbor, Michigan 48109, United States; Key Laboratory of Optoelectronics Information Technology, Ministry of Education, Tianjin University, Tianjin 300072, China; [orcid.org/0000-0002-1647-2892](https://orcid.org/0000-0002-1647-2892)

Qingyu Cui – Department of Electrical Engineering and Computer Science, University of Michigan, Ann Arbor, Michigan 48109, United States

Zhanhua Huang – Key Laboratory of Optoelectronics Information Technology, Ministry of Education, Tianjin University, Tianjin 300072, China

Complete contact information is available at:  
<https://pubs.acs.org/10.1021/acsp Photonics.9b01803>

## Notes

The authors declare the following competing financial interest(s): The approach presented in this paper is the subject of a patent application.

## ACKNOWLEDGMENTS

Z.L. acknowledges the financial support from the China Scholarship Council (CSC).

## REFERENCES

- (1) Sun, X.-D.; Liu, J.-Q. *Light emitting material integrated into a substantially transparent substrate*. U.S. Patent 6,986,581, January 17, 2006.
- (2) Liu, J.; Sun, X.-D. *System and method for a transparent color image display utilizing fluorescence conversion of nano particles and molecules*. U.S. Patent 7,090,355, August 15, 2006.
- (3) Sun, T.; Pettitt, G.; Ho, N. T.; Eckles, K.; Clifton, B.; Cheng, B.; et al. Full color, high contrast front projection on black emissive display. *Proc. SPIE* **2012**, *8254*, 82540K.
- (4) Downing, E.; Hesselink, L.; Ralston, J.; Macfarlane, R. A three-color, solid-state, three-dimensional display. *Science* **1996**, *273*, 1185–1189.
- (5) Görrn, P.; Sander, M.; Meyer, J.; Kröger, M.; Becker, E.; Johannes, H.-H.; Kowalsky, W.; Riedl, T. Towards See-Through Displays: Fully Transparent Thin-Film Transistors Driving Transparent Organic Light-Emitting Diodes. *Adv. Mater.* **2006**, *18*, 738–741.
- (6) Ju, S.; Li, J.; Liu, J.; Chen, P. C.; Ha, Y. G.; Ishikawa, F.; Chang, H.; Zhou, C.; Facchetti, A.; Janes, D. B.; Marks, T. J. Transparent active matrix organic light-emitting diode displays driven by nanowire transistor circuitry. *Nano Lett.* **2008**, *8*, 997–1004.
- (7) Park, S.-H. K.; Hwang, C. S.; Ryu, M.; Yang, S.; Byun, C.; Shin, J.; Lee, J. I.; Lee, K.; Oh, M. S.; Im, S. Transparent and photo-stable ZnO thin-film transistors to drive an active matrix organic-light-emitting-diode display panel. *Adv. Mater.* **2009**, *21*, 678–682.
- (8) Goldenberg, J. F.; McKechnie, T. S. Diffraction analysis of bulk diffusers for projection-screen applications. *J. Opt. Soc. Am. A* **1985**, *2*, 2337–2348.
- (9) Hsu, C. W.; Zhen, B.; Qiu, W.; Shapira, O.; DeLacy, B. G.; Joannopoulos, J. D.; Soljacic, M. Transparent displays enabled by resonant nanoparticle scattering. *Nat. Commun.* **2014**, *5*, 3152.
- (10) Levola, T. Diffractive optics for virtual reality display. *J. Soc. Inf. Disp.* **2006**, *14*, 467–475.
- (11) Eisen, L.; Meyklyar, M.; Golub, M.; Friesem, A. A.; Gurwich, I.; Weiss, V. Planar configuration for image projection. *Appl. Opt.* **2006**, *45*, 4005–4011.
- (12) Mukawa, H.; Akutsu, K.; Matsumura, I.; Nakano, S.; Yoshida, T.; Kuwahara, M.; Aiki, K.; Ogawa, M. A full color eyewear display using holographic planar waveguides. *Dig. Tech. Pap. - Soc. Inf. Disp. Int. Symp.* **2008**, *39*, 89–92.
- (13) Wilmington, I. K.; Valera, M. S. Waveguide-based display technology. *Dig. Tech. Pap. - Soc. Inf. Disp. Int. Symp.* **2013**, *44*, 278–280.
- (14) Liu, Z.; Pang, Y.; Pan, C.; Huang, Z. Design of a uniform-illumination binocular waveguide display with diffraction gratings and freeform optics. *Opt. Express* **2017**, *25*, 30720–30731.
- (15) Fattal, D.; Peng, Z.; Tran, T.; Vo, S.; Fiorentino, M.; Brug, J.; Beausoleil, R. G. A multi-directional backlight for a wide-angle, glasses-free three-dimensional display. *Nature* **2013**, *495*, 348–351.
- (16) Guo, L. J. Nanoimprint lithography: methods and material requirements. *Adv. Mater.* **2007**, *19*, 495–513.
- (17) Zhang, C.; Subbaraman, H.; Li, Q.; Pan, Z.; Ok, J. G.; Ling, T.; Chung, C.-J.; Zhang, X.; Lin, X.; Chen, R. T.; Guo, L. J. Printed photonic elements: nanoimprinting and beyond. *J. Mater. Chem. C* **2016**, *4*, 5133–5153.